Chaos, Solitons and Fractals 186 (2024) 115135

Contents lists available at ScienceDirect

Chaos, Solitons and Fractals

journal homepage: www.elsevier.com/locate/chaos

A variable-order fractional memristor neural network: Secure image encryption and synchronization via a smooth and robust control approach

Abdullah A. Al-Barakati [a], Fatiha Mesdoui [b], Stelios Bekiros [c,*], Sezgin Kaçar [d], Hadi Jahanshahi [e]

[a] Communication Systems and Networks Research Group, Department of Information Systems, Faculty of Computing and Information Technology, King Abdulaziz University, Jeddah, Saudi Arabia
[b] LAOTI Laboratory, Department of Mathematics, Faculty of Exact Sciences and Informatics, Mohamed Seddik Ben Yahia University, Jijel, Algeria
[c] Department of Management, University of Turin (UniTo), Italy
[d] Department of Electrical and Electronics Engineering, Faculty of Technology, Sakarya University of Applied Sciences, 54050, Sakarya, Turkey
[e] IEEE Canada, Toronto, ON, Canada

ARTICLE INFO

Keywords:
Memristor neural networks
Image encryption
Fractional calculus
Uncertain system, chatter-free control

ABSTRACT

In this research, we introduce and investigate a variable-order fractional memristor neural network, focusing on its engineering applications in synchronization and image encryption. This study stands out as a pioneering effort in proposing such an architecture for image encryption purposes. Distinct from conventional fractional-order systems, our model incorporates a time-varying fractional derivative, leading to more complex behaviors. Through numerical simulations, we vividly demonstrate the chaotic dynamics of the system. Our results further reveal the system's outstanding performance in image encryption applications. To augment the system's efficiency, we introduce a robust control strategy that guarantees smooth stabilization and synchronization of the variable-order fractional system. Considering the unique variable-order fractional nature of the system, we provide theoretical validations and empirical evidence supporting its stability and convergence properties. Additionally, we present synchronization outcomes between pairs of such neural networks employing our robust control approach. Our numerical analyses firmly substantiate the superiority of our control strategy, particularly highlighting its precision, robustness, and ability to maintain chattering-free performance under external disturbances.

1. Introduction

Over recent years, the domain of neural networks has witnessed an exponential surge in interest, propelled by their captivating applications [1–4]. A variety of neural network models, including but not limited to Hopfield, Cellular, and Cohen–Grossberg, have been instrumental in revolutionizing areas like computing technology, programming, associative memory, and image processing [5–8]. Particularly captivating for the scientific community has been the exploration of chaotic neural networks [9–11]. Some neural networks have been demonstrated to showcase chaotic behavior characterized by intricate dynamics. Given the vast application spectrum of these chaotic neural networks and their inherent unpredictable nature, there's an imperative need to innovate novel methodologies, formulate new models, and refine existing analytical techniques pertaining to these structures. As evidenced by recent literature [12–14], this area is ripe for deeper investigation and holds significant potential for future breakthroughs.

In the last four decades, scientists, mathematicians, and engineers have spent a great deal of time to the study of chaos as a fascinating nonlinear phenomenon [15–19]. The exploration has been profound and multi-dimensional, encompassing not just the theoretical intricacies but also the tangible, applied dimensions of chaos. Engineering systems stand at the forefront of this exploration. Notable areas such as nonlinear circuits, power systems protection, flow dynamics, liquid mixing processes, as well as encryption and communications, have seen chaos transition from a purely mathematical conundrum to a domain teeming with practical applications and technological potential [20–22].

In modern engineering frameworks, understanding the intricate

* Corresponding author.
E-mail addresses: aaalbarakati@kau.edu.sa (A.A. Al-Barakati), fatiha.mesdoui@univ-jijel.dz (F. Mesdoui), stelios.bekiros@unito.it (S. Bekiros), skacar@sakarya.edu.tr (S. Kaçar), jahanshahi.hadi@ieee.org (H. Jahanshahi).

https://doi.org/10.1016/j.chaos.2024.115135
Received 10 May 2024; Accepted 5 June 2024
Available online 29 June 2024

behaviors arising from chaos has proven pivotal. As nonlinearities and complexities in engineering systems grow, so does the relevance of chaos theory, providing both challenges and opportunities for innovative solutions. Whether it's in ensuring stability in power grids, optimizing fluid dynamics in industrial processes, or enhancing security in digital communications, the nuanced study of chaos continues to offer transformative insights. Moreover, the bridge between theoretical chaos research and its engineering applications promises a synergy that can drive next-generation innovations. As we advance, the interdisciplinary collaboration between mathematicians, scientists, and engineers will be essential in harnessing the full potential of chaos in solving contemporary engineering challenges and unlocking future possibilities.

A pressing challenge in real-world applications lies in devising reliable methods to model real-world phenomena. In this context, fractional calculus emerges as a potent tool, offering enhanced accuracy in the representation of such phenomena [23,24]. Consequently, fractional-order chaotic systems have garnered significant attention, especially concerning mathematical simulation and dynamical analysis [25]. While constant-order fractional derivatives offer a unique advantage in capturing a system's prolonged memory compared to integer-order derivatives, they have their limitations. Notably, they often fall short in capturing the intricacies of certain engineering and scientific events [26]. For instance, some physical systems exhibit a temporal shift in their memory properties. Recent explorations have shifted focus to the variable-order fractional (VOF) derivative, a promising approach that aptly mirrors the evolving memory characteristics of systems [27–29].

Multimedia data has seamlessly integrated into every facet of human existence, creating an intricate interplay between digital content and daily life. As technology evolves, the accessibility to digital data has skyrocketed, enabling virtually anyone to replicate and utilize it [30]. This underscores the urgency for robust frameworks to safeguard digital media [31,32]. Conventional protective measures for multimedia data falter in the face of modern digital content management challenges. Consequently, there's a compelling need to innovate and introduce more resilient methodologies and systems for the defense of digital assets [17,33,34].

The primary objective of synchronization is to align a slave system with a master system, ensuring congruence in their outputs. Given the inherent unpredictability of chaotic systems and their heightened sensitivity to minute variations in parameters and initial conditions, an extensive array of techniques has emerged for synchronizing chaotic behaviors [35,36]. In tangible physical systems or experimental contexts, chaotic dynamics often grapple with uncertain parameters, and the intrusion of external disturbances is almost inevitable. Given these challenges, robust controllers have gained prominence for their ability to manage chaotic systems. Of these, sliding mode control stands out as the premier robust control strategy, credited for its quick dynamic adaptability, resilience to parameter fluctuations, and stout defense against external perturbations [37–39]. Yet, its adoption is sometimes curtailed by the phenomenon of chattering. Often, sliding mode approaches induce unwanted chattering and oscillations in system responses, severely compromising system performance [40,41]. Consequently, the quest for a robust, chatter-free control design remains an active research frontier.

Building on the previously discussed merits of VOF derivatives in capturing dynamic memory properties, this study delves deeper into practical applications and innovations. We introduce a novel VOF neural network model, capitalizing on the inherent complexities of VOF systems, making them primed for encryption endeavors. Our research harnesses this VOF neural network to break new ground in secure image encryption. Furthermore, operational excellence is a core focus, with the introduction of a sophisticated, chatter-free control strategy. This mechanism, meticulously engineered, ensures rapid synchronization within the VOF neural network. Grounded in the sliding mode framework, it's adept at navigating the network amidst potential nonlinear, time-varying disturbances. Validated by the Lyapunov stability theorem and Barbalat's lemma, the robust convergence of our integrative system is ensured. In the following sections, these methodologies and findings will be elucidated in depth, emphasizing their implications and contributions to the field.

2. Preliminary concepts and model of the system

Since the invention of fractional calculus, several definitions for fractional derivatives have been proposed. In the current study, the Caputo definition is used for all calculations.

Definition 1. [42,43]. The Caputo fractional derivative of function $f(t)$ is defined as

$$D_t^{q_i} f(t) = \begin{cases} \dfrac{1}{\Gamma(k-q_i)} \displaystyle\int_0^t \frac{f^{(k)}(\tau)}{(t-\tau)^{q_i+1-k}} d\tau & k-1 < q_i < k \\ \dfrac{d^k}{dt^k} f(t) & q_i = k \end{cases} \tag{1}$$

where k is an integer, and $\Gamma(\cdot)$ indicates the Gamma function.

Definition 2. [42]. The fractional integral of function $f(t)$ is given by

$${}_0 I_t^{q_i} f(t) = \frac{1}{\Gamma(q_i)} \int_0^t (t-\tau)^{q_i-1} f(\tau) d\tau \tag{2}$$

In the current study, referring to the literature [44,45], we propose a VOF memristor neural network represented by the following equations:

$$D_t^{q_i(t)} x_i(t) = -c_i x_i(t) + \sum_{j=1}^{n} a_{ij}\big(x_j(t)\big) f_j\big(x_j(t)\big) + I_i \tag{3}$$

where $i = 1, 2, \ldots, n$ and n denotes the number of units in a neural network, $q_i(t)$ is the variable fractional derivative, $x_i(t)$ corresponds to the state of the ith unit at time t. Besides, c_i is a positive constant, $f_j\big(x_j(t)\big)$ represents a nonlinear function, and I_i stands for external input. In addition, $a_{ij}$is memristive connection weight, which is defined as follows

$$a_{ij}\big(x_j(t)\big) = \begin{cases} \widehat{a}_{ij} & |x_j(t)| > T_j \\ \widetilde{a}_{ij} & |x_j(t)| < T_j \end{cases} \tag{4}$$

where $\widehat{a}_{ij}$ and $\widetilde{a}_{ij}$ are constant parameters and $a_{ij}(\pm T_j) = \widehat{a}_{ij}$ or $\widetilde{a}_{ij}$. Also, T_j denotes switching jump.

For all numerical simulations, the parameters and functions of the memristive neural networks are considered as $f_j\big(x_j(t)\big) = tanh\big(x_j(t)\big)$, $n = 3, c_1 = c_2 = c_3 = -1, a_{12} = -1.2, a_{13} = 0, a_{21} = 1.8, a_{23} = 1.15$, $a_{31} = -4.75$, and $a_{32} = 0$. Also, the discontinuous parameters are:

$$\mathrm{a}_{11} = \begin{cases} 2 & |\mathrm{x}_1| < 1 \\ 2.1 & |\mathrm{x}_1| > 1, \end{cases}$$

$$\mathrm{a}_{22} = \begin{cases} 1.71 & |\mathrm{x}_2| < 1 \\ 1.89 & |\mathrm{x}_2| > 1, \end{cases}$$

$$\mathrm{a}_{33} = \begin{cases} 1.1 & |\mathrm{x}_3| < 1 \\ 0.88 & |\mathrm{x}_3| > 1, \end{cases}$$

The variable order derivative is considered to be $q_1(t) = q_2(t) = q_3(t) = 0.99 + 0.005sin(t) + 0.005cos(t)$ Figs. 1 and 2 respectively demonstrate the 2D and 3D phase portraits of the nonlinear chaotic memristive neural network.

3. Design of image encryption algorithm

In this section, an image encryption algorithm has been developed in order to demonstrate the availability of the VOF memristor neural network for data security applications. Fig. 3 shows the developed image

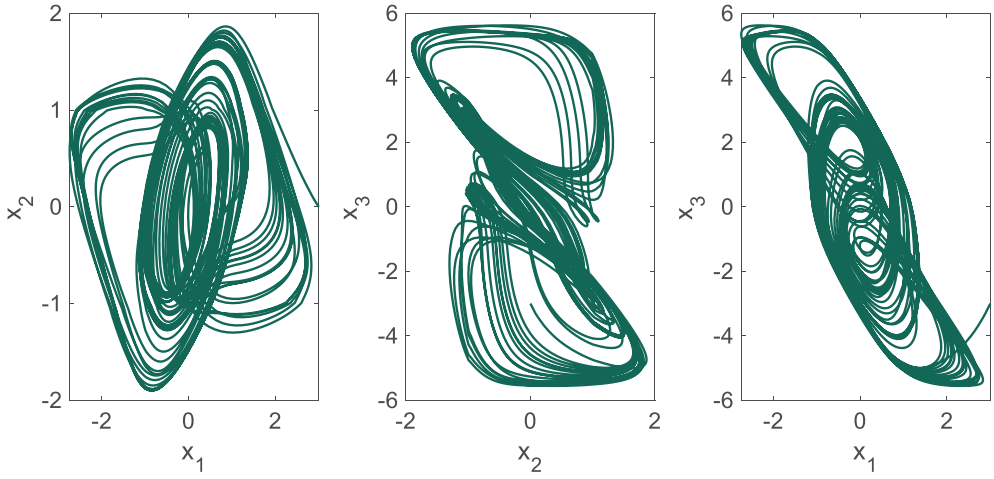

Fig. 1. 2D phase portraits of memristive neural network (3).

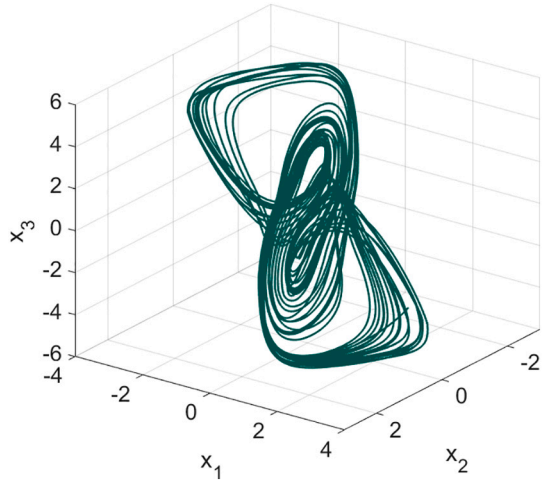

Fig. 2. 3D phase portraits of memristive neural network (3).

encryption algorithm by a flowchart.

The flowchart has two basic processes as encryption and decryption. In the encryption process, pixel values of the original image data and the numbers from state variables (x_1, $x_2$and x_3) of the new VOFmemeristorneural network are converted into binary numbers. After converting, the image data bits and the state variable bits are xored for encryption. Finally, the xored bits converted into integers for the encrypted image pixels. So, the encryption process has been finished, and the encrypted image has been obtained.

In the decryption process that is seen in the flowchart, the pixel values received from the encrypted image and the state variables (x_1, x_2 and x_3) of the VOF memristor neural network are converted to binary, and the x or operation is applied again. The obtained bits of binary numbers are converted back to integer numbers to obtain decrypted image data. At the end of the process, the decrypted image, which is the same as the original image is obtained.

4. Simulation of image encryption and security analysis

In this section, the image encryption algorithm developed in Section 3 has been performed, and the simulation results have been obtained. After that, the security analyses have been applied to simulation results.

In the simulation of the algorithm, 128 × 128 pixel size image with gray scale ("pepper") is used. Fig. 4 shows the original, encrypted and decrypted images after the simulation. As seen in Fig. 4, when the visual test has done, it can be seen that the original image and the decrypted image are the same, but the encrypted image is completely different. In addition, nothing can be understood from the encrypted image. So, it can be said that the encryption and the decryption processes are visually very successful.

Of course, testing visually does not show that the process is safe enough. Therefore, Correlation, Histogram, Entropy, and Differential Attack analyses have also been performed to show the performance of the encryption. In Table 1, the correlation, entropy and differential attack (NPCR and UACI) results show that the encryption performance is pretty good.

Correlation distributions and histogram graphs can be seen in Figs. 5 and 6, respectively. These figures demonstrate that the encryption process provides very homogeneous statistical distributions. This statistical homogeneity of the encrypted image shows that encryption is statistically very successful.

5. Controller design

Since in the model of the proposed VOF memristor neural network, $a_{ij}(x_j(t))$ has a discontinuous value, the classical definitions for differential equations cannot be applied to system (3). To overcome this problem, the concept of Filippov is used. According to Filippov [46], a differential equation with a discontinuity has the same solution as a certain differential inclusion.

Based on the theories of set-valued maps and differential inclusions [47], Eq. (3) can be rewritten as

$$D_t^{q_i(t)}x_i(t) \in -cx_i(t)\sum_{j=1}^{n} co\left(a_{ij}(x_j(t))\right)f_j(x_j(t)) + I_i \tag{5}$$

where co indicates the convex closure of $a_{ij}(x_j(t))$ and can be defined as follows

$$co\left(a_{ij}(x_j(t))\right) = \begin{cases} \widehat{a}_{ij} & |x_j(t)| > T_j \\ co\left(\widehat{a}_{ij}, \widetilde{a}_{ij}\right) & |x_j(t)| = T_j \\ \widetilde{a}_{ij} & |x_j(t)| < T_j \end{cases} \tag{6}$$

Or there exist $\gamma_{ij}(x_j(t)) \in co\left[a_{ij}(x_j(t))\right]$ such that

$$D_t^{q_i(t)}x_i(t) = -cx_i(t)\sum_{j=1}^{n}\gamma_{ij}(x_j(t))f_j(x_j(t)) + I_i \tag{7}$$

As a result, based on Ref. [46], if $x(t) = [x_1, x_2 \ldots x_n]$ is absolutely continuous on any compact interval of $[0, +\infty)$ and satisfies the differential inclusions (5) or (7), then $x(t)$ is a solution of system (3). As a result, we can use continuous model (7) instead of model (3) to design a

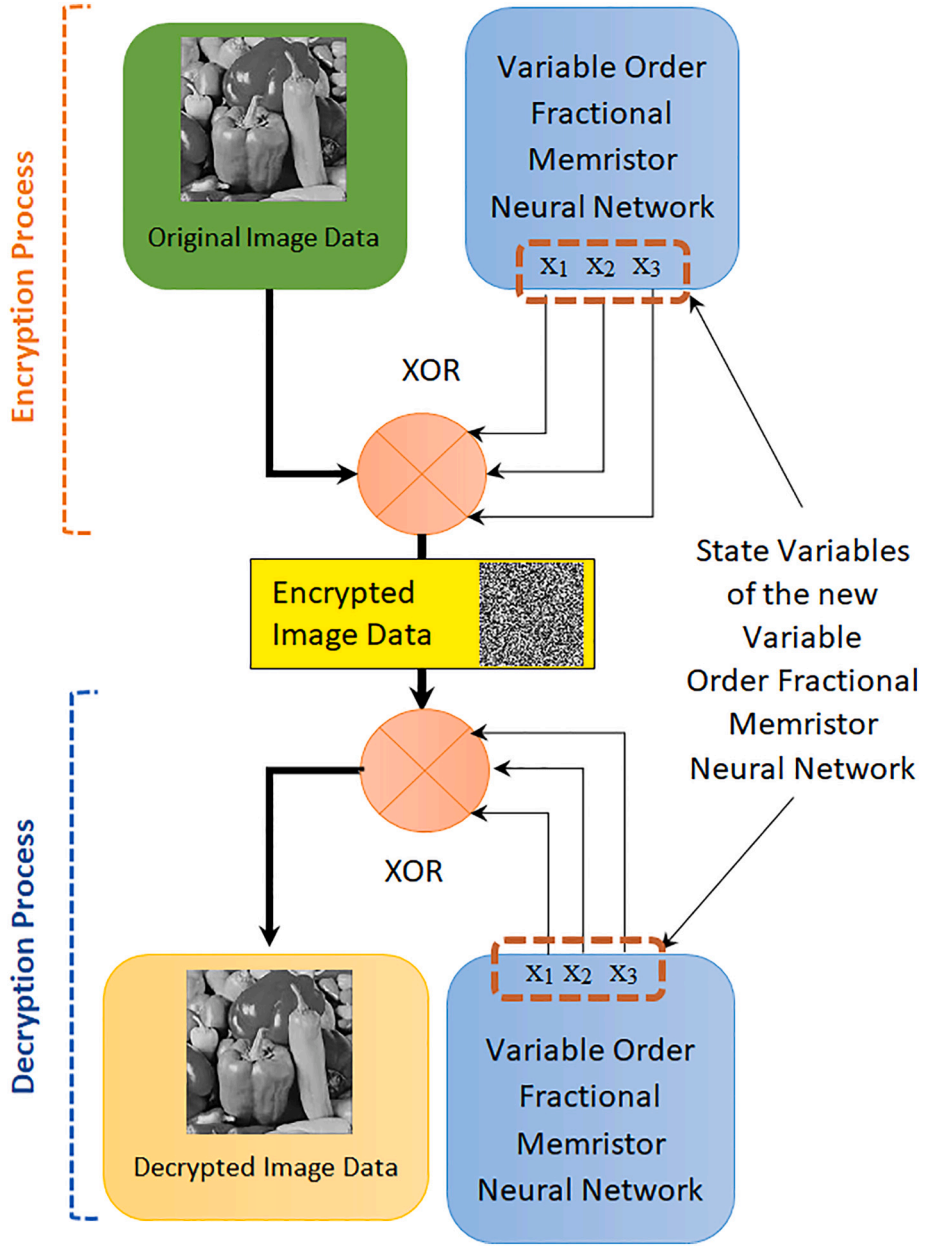

Fig. 3. Encryption and decryption processes of the image encryption.

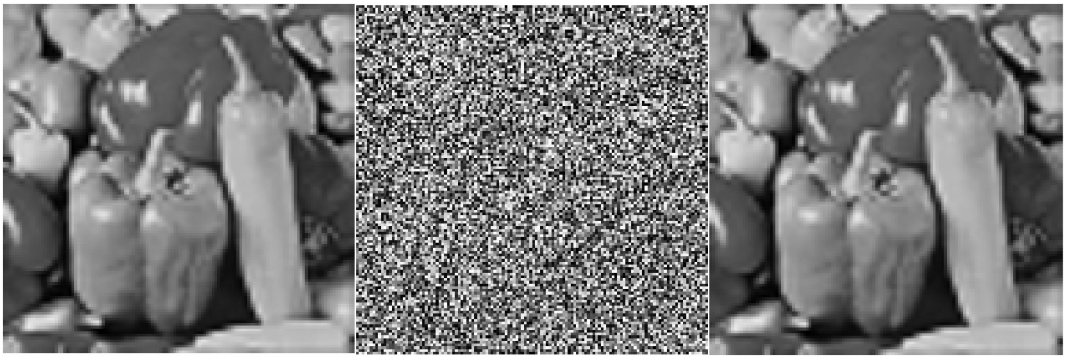

Fig. 4. Original, encrypted and decrypted images.

Table 1
Security analysis of the encryption process.

Analysis	Original image	Encrypted image
Correlation	0.9684	0.5100
Entropy	7.5875	7.9963
NPCR	99.4568	
UACI	32.8309	

controller, but the issue is that certain parameters and functions, such as γ_{ij}, are undefined in this model. As a result, implementing a reliable control scheme for such systems is of crucial importance.

Theorem 1 presents the asymptotic stability of fractional-order systems based on the Lyapunov theorem.

Theorem 1. [48]. *Consider a fractional-order nonlinear system with the following governing equation*

$$D_t^q x = f(t, x) \tag{8}$$

where $x = 0$ *is an equilibrium point of the system, the equilibrium point is asymptotically stable if there is a positive definite Lyapunov function* $V(t, x(t))$ *which satisfies the following inequality*

$$D_t^q V(t, x(t)) \leq 0 \tag{9}$$

where $q \in (0, 1)$.

Lemma 1. [49]. *For all* $t \geq t_0$ *the following nonequality is established for system (8)*

$$\frac{1}{2} D_t^q x^2(t) \leq x(t) D_t^q x(t), \forall \alpha \in (0, 1) \tag{10}$$

Provided $x(t) \in \Re$ *is a continuously differentiable function.*

In addition, Lemma 1can be extended for $x(t) \in \Re^n$. Consequently, for $\forall t \geq t_0$ we have

$$\frac{1}{2} D_t^q x^T(t) x(t) \leq x^T(t) D_t^q x(t), \forall \in (0, 1) \tag{11}$$

Theorem 2. (Barbalat's lemma) [50]. *Suppose* $\phi : \Re \to \Re$ *as a uniformly continuous function on* $[t_0, \infty)$ *which satisfies condition* $D_t^{-q} |\phi|^p \leq M$ *for all* $t > t_0 > 0$ *and constants p and M are positive. Then it is guaranteed that*

$$\lim_{t \to \infty} \phi(t) = 0 \tag{12}$$

5.1. Chatter-free and smooth control technique

Consider the master system as follows

$$D_t^{q_i(t)} y_i = g_i(t, Y) \ (i = 1, 2, \ldots, n) \tag{13}$$

Moreover, the slave system is given by

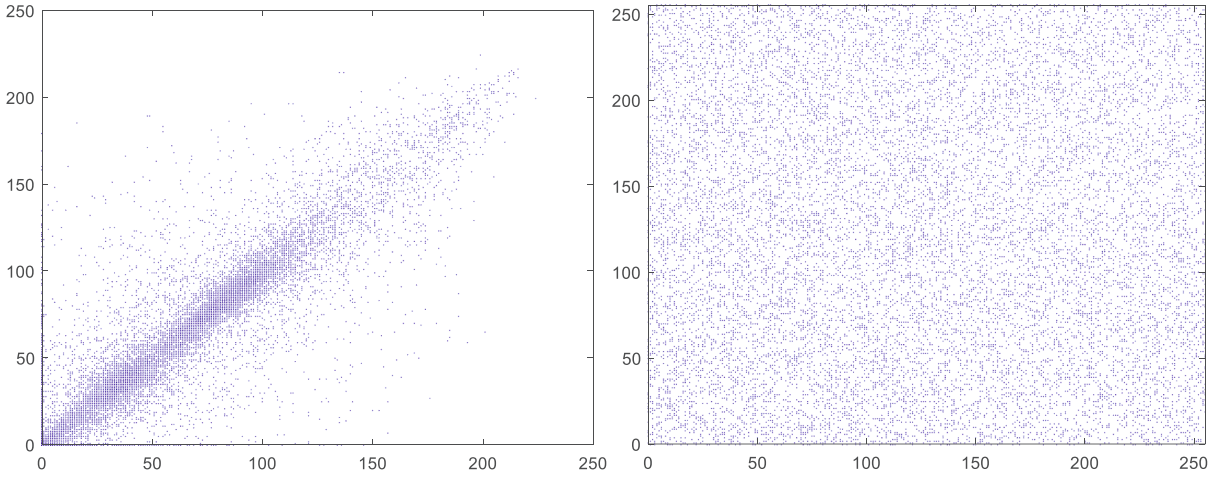

Fig. 5. Correlation distributions of original and encrypted images.

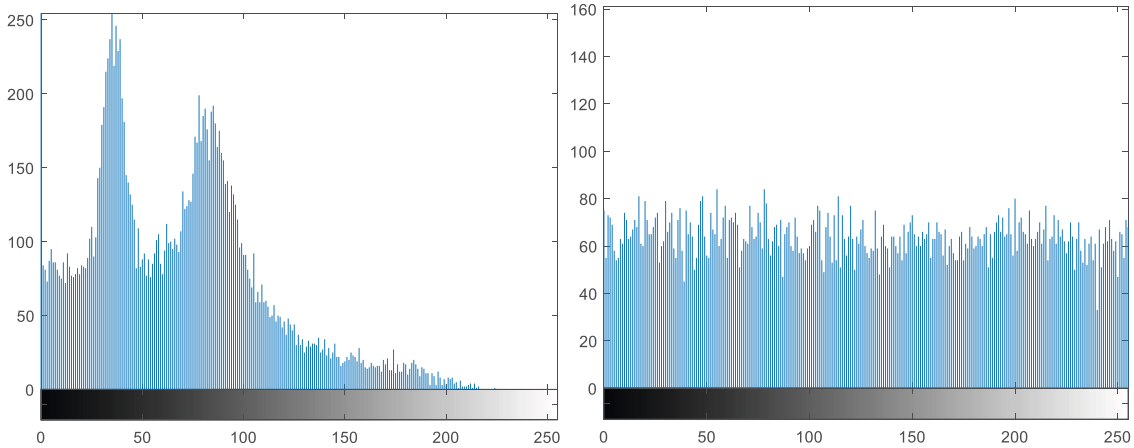

Fig. 6. Histograms of original and encrypted images.

$$D_t^{q_i(t)}x_i = f_i(t,X) + d_i(t) + u_i(t)\ (i = 1,2,\ldots,n) \tag{14}$$

where $0 < q_i(t) < 1$ is the fractional-order derivative of the equations. $Y = [y_1,\ldots,y_4]^T$ and $X = [x_1,\ldots,x_4]^T$are the measurable states of the master and slave system, respectively. $g_i(.)$and $f_i(.)$ stand for nonlinear functions of the systems. $u_i(t)$denote the control input.In addition, d_i denotes all uncertainties and external disturbance which the system experiences. We define the synchronization error as $e_i = x_i - y_i\ (i = 1,2,\ldots,n)$, consequently, we have

$$D_t^{q_i(t)}e_i = D_t^{q_i(t)}x_i - D_t^{q_i(t)}y_i = f_i(t,Y) + u_i(t) + d_i(t) - g_i(t,X)\ (i = 1,2,\ldots,n) \tag{15}$$

The sliding surface is designed as follow:

$$s_i(t) = D^{q_i(t)}e_i(t) + k_1 e_i \tag{16}$$

where k_1 is user-defined parameters that should be designed in a way that satisfies Hurwitz condition; consequently, in this case k_1 should be positive. The proposed chatter-free and smooth control law for the nonlinear uncertain VOF system is given by

$$D_t^{q_i(t)}u(t) = -\left(D_t^{q_i(t)}f_i(t,Y) - D_t^{q_i(t)}g_i(t,X) + \beta_1 sign(s_i) + \mu s_i + k_1 D_t^{q_i(t)}e_i\right) \tag{17}$$

where β_1 and $\mu$are positive user-defined parameters. Design parameters $\beta_1$should be designed based on Assumption 1.

Assumption 1. The uncertain terms and their derivatives are supposed to be bounded. The user-defined parameter $\beta_1$should be selected in a way that $\beta_1 > \left|D_t^{q_i(t)}d_i(t)\right|$.

Remark 1. In the proposed control law, we intend to provide a smooth and chatter-free control input by transferring discontinuous function sign(.) to the fractional derivative of the control signal instead of itself. Indeed, the discontinuous function $sign(.)$, which is transferred to the derivative of the control input, will provide smooth and chatter-free results.

Theorem 3. *Under offered control law (17), the tracking error of the nonlinear VOF system (15) converges to zero even where there are time-varying uncertainties and disturbances.*

Proof. Consider the following Lyapunov function

$$V(t) = \frac{1}{2}\sum_{i=1}^{n} s_i^2. \tag{18}$$

Based on the Lemma 1 by taking the time derivative of the Lyapunov function, we have

$$\begin{aligned} D_t^{q_i(t)}V(t) &\le \sum_{i=1}^{n} s_i D_t^{q_i(t)}s_i = \sum_{i=1}^{n} s_i D_t^{q_i(t)}\left(D_t^{q_i(t)}e_i(t) + k_1 e_i\right) \\ &= \sum_{i=1}^{n} s_i\left(D_t^{q_i(t)}f_i(t,Y) + D^q u_i(t) + D^q d_i(t) - D^q g_i(t,X) + k_1 D_t^{q_i(t)}e_i\right) \end{aligned} \tag{19}$$

Substituting the proposed control law (17), we have

$$D_t^{q_i(t)}V(t) \le \sum_{i=1}^{n} s_i\left(-\beta_1 sign(s_i) - \mu s_i + D_t^{q_i(t)}d_i(t)\right) \tag{20}$$

Based on Assumption 1, we reach

$$D_t^{q}V(t) \le \sum_{i=1}^{n} -\mu s_i^2 \tag{21}$$

integrating both sides of Eq. (21) yields

$$\begin{aligned} D_t^{-q}D_t^{q}V = V(t) - V(0) \le -D_t^{-q}\sum_{i=1}^{n}\mu s_i^2 = \sum_{i=1}^{n} -\mu D_t^{-q}\left(|s_i|^2\right) \\ \Rightarrow V(t) + \sum_{i=1}^{n}\mu D_t^{-q}\left(|s_i|^2\right) \le V(0) \end{aligned} \tag{22}$$

Since $V(t)$ is a positive definite function, one can achieve

$$\sum_{i=1}^{n}\mu D_t^{-q}\left(|s_i|^2\right) \le V(0) \Rightarrow \sum_{i=1}^{n} D_t^{-q}\left(|s_i|^2\right) \le \frac{V(0)}{\mu} \tag{23}$$

On the basis of Theorem 1 and 2 as well as Eqs. (21) and (23), the error of the system converges to the sliding surface; consequently, the error of synchronization asymptotically converges to zero. Also, since the proposed control signal $u(t)$is calculated through an integral filter, the response of the system will be chatter-free and smooth.

6. Simulation results of synchronization

In this section, numerical results of synchronization of the uncertain system which is carried out using MATLAB, are shown. System (3) is considered to be the master system. Also, the slave system is considered as follows

$$D^{q_i(t)}y_i(t) = -c_i y_i(t) + \sum_{j=1}^{n} a_{ij}\left(y_j(t)\right)f_j\left(y_j(t)\right) + I_i + d_i + u_i \tag{24}$$

The parameters of both the master and slave systems are the same and are equal to what is mentioned in Section 2, while the initial conditions of the slave and master system are different, i.e., $Y_0 = [0,-1,0]^T$and $X_0 = [-1.5,0,0]^T$. Time-varying unknown external disturbances are considered as

$$d_1(t) = d_2(t) = d_3(t) = 0.5sin(t) + 0.5cos(t) \tag{25}$$

The user-defined parameters of the controller are designed as $\mu = [2, 2.5, 1.5]$, $\beta_1 = [3.6, 2.5, 3]$, $k_1 = [10, 10, 10]$.

Fig. 7 displays the time-history evolution of both the master and slave systems. Observing the traces, it becomes evident that even amidst the presence of time-varying unknown disturbances, the slave system is adept at tracking the trajectory of the master system. The controller is activated at $T = 5$, and by $T = 10$ (after 5 normalized time units), the slave system exhibits significant alignment with the master system. This synchronization is not only achieved swiftly but is also sustained throughout the observed duration, spanning from 10 to 80 units of normalized time. Fig. 8 demonstrates a quantified perspective on the synchronization errors, denoted as e_1, e_2, and e_3. Each of the plots presents an initial perturbation in error, likely attributed to the system's inherent dynamics and the transient effects. However, post this transitory phase, a clear pattern emerges across all three plots. By the aforementioned 10-unit mark, each synchronization error converges to a near-zero steady state, a testament to the efficacy of the

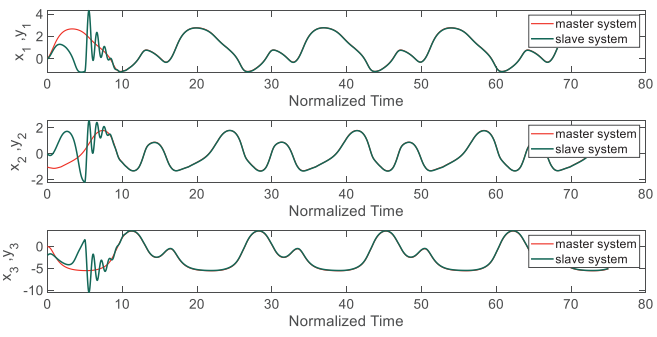

Fig. 7. Time history of synchronization results based on the offered control technique (the controller is turned on at $t = 5$).

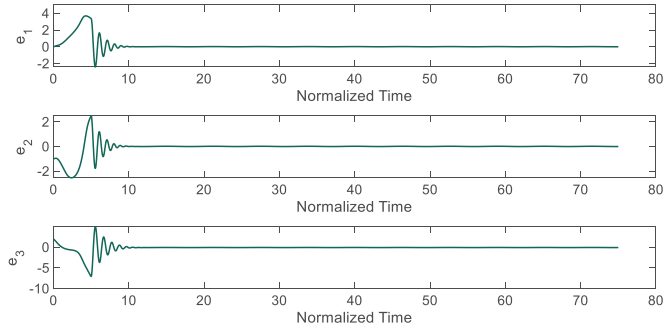

Fig. 8. The error of synchronization based on the offered control technique (the controller is turned on at $t = 5$).

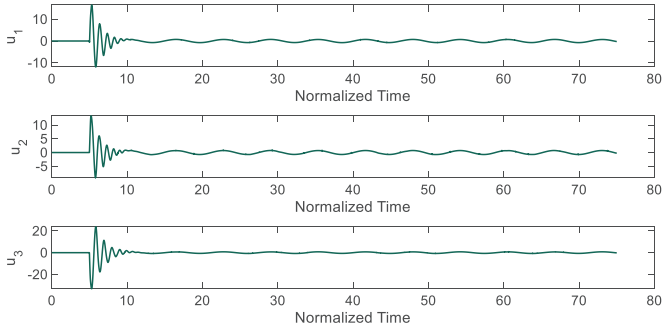

Fig. 9. The control signal based on the offered control technique (the controller is turned on at $t = 5$).

synchronization mechanism employed. The consistently low values of e_1, e_2, and $e_3$post this point underscores the robustness of the synchronization process, even in the face of initial system disturbances. In summary, together, these figures validate the robustness and efficiency of synchronization, making a compelling case for its applicability in real-world scenarios where precise synchronization is imperative.

Fig. 9 displays the applied control signals. As it is shown in this figure each plot shows significant activity up to $T = 10$. This activity is indicative of the transient responses as the control system endeavors to align the system's state with the desired trajectory. After this phase, each control input demonstrates a consistent trend, indicating the system's progression to a steadier operational state. Furthermore, the control inputs are seamless, devoid of chatter, and have well-regulated amplitudes. This underscores the controller's expertise in handling system dynamics, ensuring both stability and precision.

A salient feature of the depicted control signals is their smooth nature throughout the observation period, highlighting the absence of chatter in the control strategy. Chatter, a common challenge in control systems, can lead to premature wear of system components, and its omission in Fig. 9 is noteworthy. Additionally, the trajectories of u_1, u_2, and u_3 remain devoid of erratic surges or oscillations, reinforcing the resilience of the system against potential disturbances.

In summary, the synchronization simulations explicitly support the proposed control scheme's accurate and chatter-free performance. As a result, the suggested control scheme could be used to control and synchronize a wide variety of nonlinear uncertain VOF systems.

7. Conclusion

In this study, we presented a chaotic memristor neural network. By capitalizing on the characteristics of time-varying fractional derivatives, the VOF scheme attains enhanced degrees of freedom. This not only boosts the system's adaptability but also positions the VOF framework uniquely for roles in data transfer and information security. Leveraging these beneficial features, we introduced an image encryption scheme based on the proposed VOF. When examining the image encryption outcomes, it became evident that our VOF framework secured images capably, recording remarkable levels of encryption as highlighted by the Correlation, Histogram, Entropy, and Differential Attack assessments. Further, we presented an innovative controller, meticulously crafted to fine-tune synchronization between the master and slave configurations. Employing the proposed controller, the slave system showcased an outstanding ability to shadow the master system's trajectory, even when confronted with unpredictable, time-varying disturbances. This prowess was substantiated as synchronization errors trended towards minimal values, with control inputs stabilizing after initial transient events and characterized by an absence of chatter and controlled amplitude fluctuations. In light of these findings, our methodology offers substantial capabilities in both secure data conveyance and achieving meticulous synchronization in demanding scenarios. Peering into the future, given the complex nature of our chaotic memristor neural network, intertwining the VOF design with advanced adaptive learning mechanisms or segmented neural designs could further enhance encryption resilience and synchronization accuracy, paving the way for an integrated system adeptly geared to adapt to shifting data landscapes and unforeseen system perturbations.

CRediT authorship contribution statement

Abdullah A. Al-Barakati: Data curation, Investigation, Methodology, Software, Writing – original draft. **Fatiha Mesdoui:** Data curation, Software, Validation, Visualization. **Stelios Bekiros:** Conceptualization, Data curation, Investigation, Methodology, Project administration, Supervision, Validation, Writing – review & editing. **Sezgin Kaçar:** Formal analysis, Resources, Software, Validation, Writing – original draft, Writing – review & editing. **Hadi Jahanshahi:** Conceptualization, Data curation, Investigation, Methodology, Project administration, Resources, Software, Supervision, Validation, Visualization, Writing – original draft, Writing – review & editing.

Declaration of competing interest

The authors declare that they have no known competing financial interests or personal relationships that could have appeared to influence the work reported in this paper.

Data availability

Data will be made available on request.

Acknowledgement

This research work was funded by Institutional Fund Projects under grant no. (IFPIP: 596-611-1443). The authors gratefully acknowledge technical and financial support provided by the Ministry of Education and King Abdulaziz University, DSR, Jeddah, Saudi Arabia.

References

[1] Nielsen MA. Neural networks and deep learningvol. 25. CA, USA: Determination press San Francisco; 2015.
[2] Jahanshahi H, Castillo O. PREFACE: application of artificial intelligence in tracking control and synchronization of spacecraft. Adv Space Res 2023;71:3533.
[3] Bishop CM. Neural networks and their applications. Review of Scientific Instruments 1994;65:1803–32.
[4] Jahanshahi H, Castillo O, Yousefpour A. Chaotic variable-order fractional neural networks. Springer; 2022.
[5] Barra A, Beccaria M, Fachechi A. A new mechanical approach to handle generalized Hopfield neural networks. Neural Netw 2018;106:205–22.
[6] Guo Y. Exponential stability analysis of travelling waves solutions for nonlinear delayed cellular neural networks. Dynamical Systems 2017;32:490–503.
[7] Wen U-P, Lan K-M, Shih H-S. A review of Hopfield neural networks for solving mathematical programming problems. European Journal of Operational Research 2009;198:675–87.

[8] Chen T, Rong L. Delay-independent stability analysis of Cohen–Grossberg neural networks. Physics Letters A 2003;317:436–49.
[9] Ganesan B, Annamalai M. Anti-synchronization analysis of chaotic neural networks using delay product type looped-Lyapunov functional. Chaos, Solitons & Fractals 2023;174:113898.
[10] Sheng S, Wang X. Network traffic anomaly detection method based on chaotic neural network. Alex Eng J 2023;77:567–79.
[11] Rahatabad FN, Sheikhani A, Dabanloo NJ. A chaotic neural network model for biceps muscle based on Rossler stimulation equation and bifurcation diagram. Biomedical Signal Processing and Control 2022;78:103852.
[12] Aihara K. Chaos engineering and its application to parallel distributed processing with chaotic neural networks. Proc IEEE 2002;90:919–30.
[13] Lahmiri S, Bekiros S. Cryptocurrency forecasting with deep learning chaotic neural networks. Chaos, Solitons & Fractals 2019;118:35–40.
[14] Cao J, Alofi A, Al-Mazrooei A, Elaiw A. Synchronization of switched interval networks and applications to chaotic neural networksvol. 2013. Hindawi; 2013.
[15] Yousefpour A, Haji Hosseinloo A, Reza Hairi Yazdi M, Bahrami A. Disturbance observer–based terminal sliding mode control for effective performance of a nonlinear vibration energy harvester. Journal of Intelligent Material Systems and Structures 2020;31:1495–510.
[16] Aguirre LA. Letellier C. Modeling Nonlinear Dynamics and Chaos: A review. Mathematical Problems in Engineering; 2009. p. 2009.
[17] Jahanshahi H, Yousefpour A, Munoz-Pacheco JM, Kacar S, Pham V-T, Alsaadi FE. A new fractional-order hyperchaotic memristor oscillator: dynamic analysis, robust adaptive synchronization, and its application to voice encryption. Appl Math Comput 2020;383:125310.
[18] Wei Z, Yousefpour A, Jahanshahi H, Kocamaz UE, Moroz I. Hopf bifurcation and synchronization of a five-dimensional self-exciting homopolar disc dynamo using a new fuzzy disturbance-observer-based terminal sliding mode control. J Franklin Inst 2021;358:814–33.
[19] Yousefpour A, Vahidi-Moghaddam A, Rajaei A, Ayati M. Stabilization of nonlinear vibrations of carbon nanotubes using observer-based terminal sliding mode control. Transactions of the Institute of Measurement and Control 2020;42:1047–58.
[20] Yousefpour A, Jahanshahi H, Munoz-Pacheco JM, Bekiros S, Wei Z. A fractional-order hyper-chaotic economic system with transient chaos. Chaos, Solitons & Fractals 2020;130:109400.
[21] Jahanshahi H, Yousefpour A, Wei Z, Alcaraz R, Bekiros S. A financial hyperchaotic system with coexisting attractors: dynamic investigation, entropy analysis, control and synchronization. Chaos, Solitons & Fractals 2019;126:66–77.
[22] Yousefpour A, Bahrami A, Haeri Yazdi MR. Multi-frequency piezomagnetoelastic energy harvesting in the monostable mode. Journal of Theoretical and Applied Vibration and Acoustics 2018;4:1–18.
[23] Chen S-B, Jahanshahi H, Abba OA, Solís-Pérez J, Bekiros S, Gómez-Aguilar J, et al. The effect of market confidence on a financial system from the perspective of fractional calculus: numerical investigation and circuit realization. Chaos, Solitons & Fractals 2020;140:110223.
[24] Chen S-B, Rajaee F, Yousefpour A, Alcaraz R, Chu Y-M, Gómez-Aguilar J, et al. Antiretroviral therapy of HIV infection using a novel optimal type-2 fuzzy control strategy. Alex Eng J 2021;60:1545–55.
[25] Chu Y-M, Bekiros S, Zambrano-Serrano E, Orozco-López O, Lahmiri S, Jahanshahi H, et al. Artificial macro-economics: a chaotic discrete-time fractional-order laboratory model. Chaos, Solitons & Fractals 2021;145:110776.
[26] Sun H, Chen W, Wei H, Chen Y. A comparative study of constant-order and variable-order fractional models in characterizing memory property of systems. The European Physical Journal Special Topics 2011;193:185–92.
[27] Singh AK, Mehra M, Gulyani S. Learning parameters of a system of variable order fractional differential equations. Numerical Methods for Partial Differential Equations 2023;39:1962–76.
[28] Patnaik S, Hollkamp JP, Semperlotti F. Applications of variable-order fractional operators: a review. Proceedings of the Royal Society A 2020;476:20190498.
[29] Zhang R, Mao S, Kang Y. A novel traffic flow prediction model: variable order fractional grey model based on an improved grey evolution algorithm. Expert Systems with Applications 2023;224:119943.
[30] Granello DH, Wheaton JE. Online data collection: strategies for research. J Couns Dev 2004;82:387–93.
[31] Dang PP, Chau PM. Image encryption for secure internet multimedia applications. IEEE Transactions on Consumer Electronics 2000;46:395–403.
[32] Yang M, Bourbakis N, Li S. Data-image-video encryption. IEEE Potentials 2004;23:28–34.
[33] Ahmad M, Alam B, Farooq O. Chaos based mixed keystream generation for voice data encryption. arXiv Preprint arXiv:14034782 2014.
[34] Nguyen N, Pham-Nguyen L, Nguyen MB, Kaddoum G. A low power circuit design for chaos-key based data encryption. IEEE Access 2020;8:104432–44.
[35] Jahanshahi H, Yousefpour A, Munoz-Pacheco JM, Moroz I, Wei Z, Castillo O. A new multi-stable fractional-order four-dimensional system with self-excited and hidden chaotic attractors: dynamic analysis and adaptive synchronization using a novel fuzzy adaptive sliding mode control method. Appl Soft Comput 2020;87:105943.
[36] Bekiros S, Jahanshahi H, Bezzina F, Aly AA. A novel fuzzy mixed H2/H∞ optimal controller for hyperchaotic financial systems. Chaos, Solitons & Fractals 2021;146:110878.
[37] Jahanshahi H, Yao Q, Alotaibi ND. Fixed-time nonsingular adaptive attitude control of spacecraft subject to actuator faults. Chaos, Solitons & Fractals 2024;179:114395.
[38] Jahanshahi H. Smooth control of HIV/AIDS infection using a robust adaptive scheme with decoupled sliding mode supervision. The European Physical Journal Special Topics 2018;227:707–18.
[39] Shtessel Y, Edwards C, Fridman L, Levant A. Sliding mode control and observationvol. 10. Springer; 2014.
[40] Wan S, Li X, Su W, Yuan J, Hong J. Active chatter suppression for milling process with sliding mode control and electromagnetic actuator. Mechanical Systems and Signal Processing 2020;136:106528.
[41] Li H, Liao X, Li C, Li C. Chaos control and synchronization via a novel chatter free sliding mode control strategy. Neurocomputing 2011;74:3212–22.
[42] Kai D. The analysis of fractional differential equations: an application-oriented exposition using differential operators of Caputo type. Lecture Notes in Mathematics, Springer 2010.
[43] Caputo M. Linear models of dissipation whose Q is almost frequency independent—II. Geophys J Int 1967;13:529–39.
[44] Lin H, Wang C, Hong Q, Sun Y. A multi-stable memristor and its application in a neural network. IEEE Trans Circuits Syst II Express Briefs 2020;67:3472–6.
[45] Thomas A. Memristor-based neural networks. J Phys D Appl Phys 2013;46:093001.
[46] Filippov AF. Differential equations with discontinuous righthand sides: Control systemsvol. 18. Springer Science & Business Media; 2013.
[47] Aubin J-P, Cellina A. Differential inclusions: Set-valued maps and viability theoryvol. 264. Springer Science & Business Media; 2012.
[48] Jarad F, Abdeljawad T, Baleanu D. Stability of q-fractional non-autonomous systems. Nonlinear Analysis: Real World Applications 2013;14:780–4.
[49] Aguila-Camacho N, Duarte-Mermoud MA, Gallegos JA. Lyapunov functions for fractional order systems. Communications in Nonlinear Science and Numerical Simulation 2014;19:2951–7.
[50] Zhang R, Liu Y. A new Barbalat's lemma and Lyapunov stability theorem for fractional order systems. IEEE 2017:3676–81.